Chapter 3
Surface Pressure Reconstruction in Shock Tube Tests Using the Virtual Fields Method

R. Kaufmann, E. Fagerholt, and V. Aune

Abstract This study investigates full-field, dynamic pressure reconstruction during shock-structure interactions using optical measurements and the virtual fields method (VFM). Shock wave impacts pose severe challenges to experimental measurement techniques due to the substantial, almost instantaneous pressure rises they induce. Their effects are typically measured pointwise using pressure transducers or as total force using load cells. Here, surface deformations were measured on the blind side of a flat steel plate in pure bending using a deflectometry setup. Pressure was reconstructed from the deformations induced by an impacting shock wave using a piecewise VFM approach. Different shock wave symmetries were used in order to investigate the capabilities of identifying spatial distributions reliably under the experimental conditions in the shock tube. Pointwise pressure transducer measurements allowed a validation of the results. It was found that different shapes of load distributions on the sample surface can be identified qualitatively, but that the comparability of both measurement techniques is limited due to filter and sampling capabilities.

Keywords Pressure reconstruction · Virtual fields method · Full-field measurement · Shock wave · Fluid-structure interaction

3.1 Introduction

Shock tube experiments are favourable to obtain a better understanding of shock-structure interaction and may therefore be used in the development of resilient structures prone to extreme loading events. In order to improve the design of protective and resilient structures, both material behaviour and fluid-structure interactions occurring during extreme loading events are subject to current research [1, 2]. While structural responses can often be measured in full-field using DIC, load distributions during impact are usually assessed pointwise using pressure transducers. This does not allow detailed investigations of the fluid-structure interactions due to the resulting low spatial resolution of pressure data and the intrusive nature of such transducers. Available full-field techniques are generally limited in terms of their applicability, as discussed in the following. If the flow field is accessible, particle image velocimetry (PIV) and particle tracking velocimetry (PTV) allow full-field pressure reconstruction in the flow over a large range of pressure amplitudes [3, 4]. In extreme flow environments involving compressible effects like shock waves, these methods are generally not applicable because the gas bubbles that are used as tracer particles burst and only a limited number of window elements can be installed for optical access. Pressure-sensitive paints [5, 6] are often used for the measurement of large differential pressure amplitudes surfaces, but they also require optical access to the pressure side of the structure under consideration, which is often challenging. New approaches are required to achieve full-field measurements of surface loads in extreme flow environments. Addressing this gap, the present study aims at applying an approach for optically measuring deformations and then reconstructing the load distributions occurring during the impact of a shock wave on a flat, thin steel plate. Using thin plate samples in pure bending allows employing the Kirchoff-Love theory which relates the involved deformations to the acting loads [7]. The main limitation of this method is that it

R. Kaufmann (✉)
Structural Impact Laboratory (SIMLab), Department of Structural Engineering, NTNU – Norwegian University of Science and Technology, Trondheim, Norway
e-mail: rene.kaufmann@ntnu.no

E. Fagerholt · V. Aune
Structural Impact Laboratory (SIMLab), Department of Structural Engineering, NTNU – Norwegian University of Science and Technology, Trondheim, Norway

Centre for Advanced Structural Analysis (CASA), NTNU, Trondheim, Norway

S. L. B. Kramer et al. (eds.), *Thermomechanics & Infrared Imaging, Inverse Problem Methodologies, Mechanics of Additive & Advanced Manufactured Materials, and Advancements in Optical Methods & Digital Image Correlation, Volume 4*, Conference Proceedings of the Society for Experimental Mechanics Series, https://doi.org/10.1007/978-3-030-86745-4_3

involves fourth-order spatial derivatives and second-order temporal derivatives of the deflections, which tend to significantly amplify experimental noise. This issue can be addressed by using the virtual fields method (VFM). The VFM is an application of the principle of virtual work and relies on using full-field deformations and material constitutive mechanical parameters to extract load information or vice versa [8]. In case of thin plates in pure bending, employing the principle of virtual work reduces the required order of spatial derivatives of deflections to two. The VFM requires the choice of appropriate virtual fields which are subject to current research. The present study utilizes a VFM approach based on piecewise virtual fields in combination with deflectometry, a highly sensitive optical technique that allows measuring surface slopes [9]. These techniques were previously combined to reconstruct dynamic mechanical point loads [10]. Pressure reconstructions of air jets impinging on a thin glass mirror were investigated in a series of studies [11–13]. In these previous studies it was found that shapes, locations and time histories of the relatively small external loads of ca. 10–1000 Pa could be identified qualitatively well, but that the accuracy of the approach is highly dependent on signal-to-noise ratio, experimental bias and processing parameters. Simulated experiments were conducted in [11] to assess the accuracy of static reconstruction results. The present study applies this methodology to shock waves impacting steel plates to investigate its capabilities in this extreme experimental environment in terms of potential experimental bias from vibrations, temporal and spatial resolution. Two shock wave symmetries are used to demonstrate the performance of the technique to capture dynamic, spatial full-field distributions. The results are compared to pressure transducer measurements to evaluate the achieved accuracy in pressure amplitude.

3.2 Deflectometry

Deflectometry is an optical measurement technique for surface slopes [9]. As illustrated in Fig. 3.1, the basic setup consists of a specimen with specular reflective surface, a cross-hatched grid with printed pitch p_G, a camera and a light source. The camera is placed at an angle next to the printed grid such that it records the reflected grid in normal incidence. The angle should be minimized to avoid distortions in the recorded image. Here, both grid and camera are placed at a distance h_G from the specimen surface. As shown in Fig. 3.1, a camera pixel records the reflected grid point P when directed at point M on the specimen surface when no load is applied. If the specimen is loaded, it deforms and local changes of the surface slopes, d α, occur. For sufficiently small deformations rigid body movements and out-of-plane deflections can be neglected and the pixel directed at point M records the reflected grid point P′ when a load is applied. Phase detection algorithms allow an extraction of local phase information from grid images and further the phase shift that results from applying a load to the specimen. Here, phase maps were applied using a spatial phase-stepping algorithm [14]. A detection algorithm featuring a windowed discrete Fourier transform algorithm with triangular weighting was employed as it can suppress some harmonics and errors from miscalibration. A detection kernel size of two grid pitches is used in this study. The displacement, u, between points P and P′ is

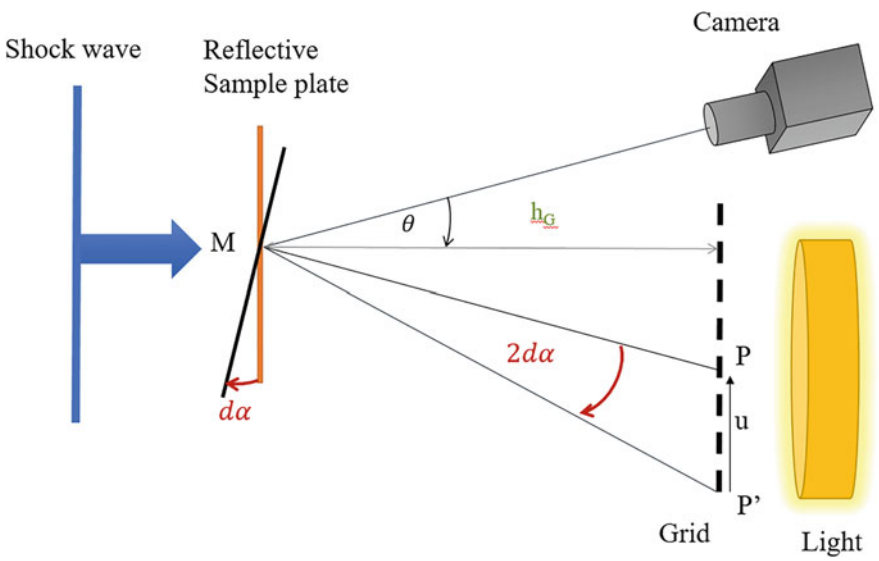

Fig. 3.1 Sketch of a deflectometry setup with specular reflective sample plate and basic principles

then obtained from the difference in phase maps between loaded and unloaded configuration. A linear relation between surface slopes d α and measured displacement u can be derived based on geometrical considerations. Assuming that h_G is large against u and the specimen dimensions, θ is negligible and that the camera records images in normal incidence, dx can be expressed as:

$$d\alpha_x = \frac{u_x}{2h_G}, d\alpha_y = \frac{u_y}{2h_G} \tag{3.1}$$

A more complicated, full calibration is required if these assumptions are not accurate [15]. The printed grid pitch, p_G, drives the resolution in both space and slope. The slope resolution is further driven by measurement noise and the distance between grid and sample surface, h_G.

3.3 Pressure Reconstruction

Based on the principle of virtual work, the VFM is a technique that allows identifying surface pressure loads from full-field kinematic measurements and known constitutive material parameters or vice versa [8]. It is computationally cheap when compared to alternative approaches like Finite Element Model updating because it does not rely on iterative procedures to match numerical and experimental results. Further, it does not require knowledge of the boundary conditions. Here, the curvatures and accelerations obtained from deflectometry measurements were used to reconstruct pressure via the principle of virtual work for a thin plate in pure bending. Eq. (3.2) describes the equilibrium of an isotropic, homogeneous plate through the principle of virtual work, assuming pure bending and linear elasticity.

$$\int_S p(t_i) \cdot w^* dS = \int_S \kappa^* D\kappa(t_i) dS + \int_S \rho t \, a(t_i) \, w^* dS \tag{3.2}$$

p is the investigated pressure, t_i a point in time, S the surface area of the element, D the bending stiffness matrix, κ the curvature and a the acceleration. w^* and κ^* are the virtual deflections and curvatures, with conditions that $\boldsymbol{w}^*$ is continuous, differentiable with continuous derivatives. Curvatures were obtained using a central difference differentiation scheme. In order to obtain accelerations, deflections were first calculated using a sparse matrix integration scheme. Acceleration were then calculated using a 5-point central difference temporal differentiation scheme. Since the material parameters are known a priori, p can then be identified once suitable virtual fields are chosen. 4-node hermite 16 element shape functions as used in the finite element method [11] are well suited here because they provide C^1 continuity of $\boldsymbol{w}^*$ and therefore C^0 continuity of the virtual slopes [9, chap. 15]. Pressure is reconstructed within a window of four hermite elements of a chosen size. Pressure is then reconstructed piecewise by shifting the window over the investigated field of view. The size of the pressure reconstruction window (PRW) is a key reconstruction parameter. Another key parameter is the slope filter kernel size. Slope filtering is conducted using a 3D gaussian filter to obtain curvature and acceleration maps that are sufficiently smooth for pressure reconstruction. The kernel size σ is defined as one standard deviation of the Gaussian. In the present study, a pressure reconstruction window with a side length of PRW = 30 data points and a slope filter kernel of $\sigma = 2$ were used. The PRW was shifted by one data point in each direction over the entire field of view. This leads to spatial oversampling of the experimental data but was found to significantly improve the results at acceptable computational cost.

3.4 Experimental Methods

The experiments were conducted in a shock tube designed for the simulation of blast waves [16]. A half blockage was added to the square nozzle exit with 300 mm side length in order to vary the symmetry of the shock wave, thus allowing an investigation of the capabilities to measure the resulting difference in pressure amplitude and history on the specimen surface. The specimen, a 300 mm square steel plate with fully clamped boundary conditions, was mounted on a rigid frame that was constructed to assure that no out-of-plane motion of the sample would occur during the experiment. Further, a wind shield was installed around the sample frame to protect the camera and grid required for the deflectometry setup. Both camera and grid were mounted on a separate frame inside the shock tube test chamber. Even though deflectometry is highly sensitive to vibrations in both camera and grid, all parasitic vibrations were assumed to occur several milliseconds after the shock wave reaches the sample plate, allowing for an accurate measurement for the duration of the initial impact on the specimen.

Table 3.1 Experimental parameters

Sample	Mirror polished steel 1.4301
Sample Young's modulus	200 GPa
Sample density	8 g cm^{-3}
Sample Poisson's ratio	0.3
Sample thickness	5 mm
Sample side length	300 mm
Sample boundary conditions	Clamped
Camera	Phantom v2511
Frame rate	75 kHz
Resolution	512 pixels × 512 pixels
Shutter speed	5 μs
Distance camera-sample	1.37 m
Printed grid pitch	5.88 mm

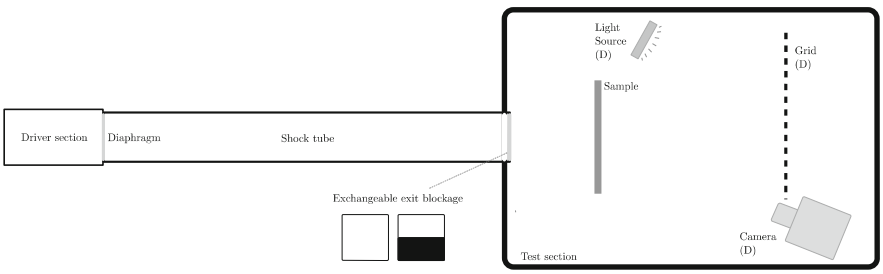

Fig. 3.2 Shock tube and deflectometry setup

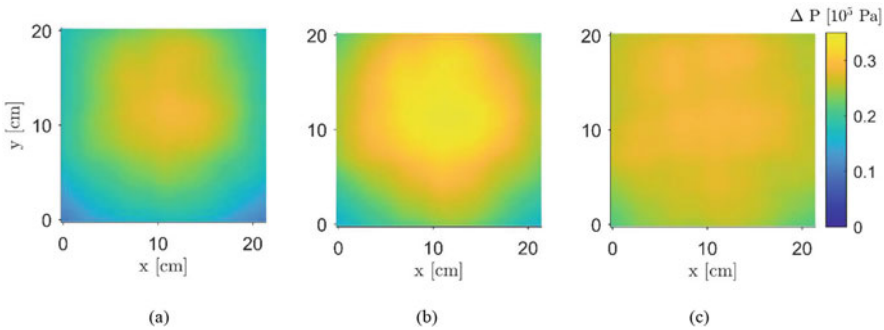

Fig. 3.3 Pressure reconstructions for open nozzle exit test case. Reconstruction at t = 0.1 ms (**a**), t = 0.14 ms (**b**), t = 0.18 ms (**c**)

Table 3.1 shows the relevant experimental parameters. Figure 3.2 shows a sketch of the setup. Additionally, pressure transducer measurements were conducted using a Kistler Type 603B sensor. For this purpose, the mirror specimen was replaced with a 2 cm thick aluminium plate with a pressure transducer placed in the centre.

3.5 Analysis

Figures 3.3 and 3.4 show reconstructed pressure maps for the two investigated cases of open and half-blocked nozzle exits. In case of the open nozzle exit, a nearly gaussian distribution is observed at all shown time steps at varying amplitude. With the bottom half of the nozzle exit blocked, the shock wave impacts the top of the plate first and induces lower peak pressure amplitudes. At later time steps, it is found that the peak pressure area propagates downwards at decreasing amplitude. The reconstructions allow an identification of the different shapes and amplitudes at all investigated time steps. It should be noted that during the time steps of initial impact shown here, inertial forces govern the dynamics, such that the accelerations extracted from deflectometry data are the most relevant quantity in terms of measurement. Figure 3.5 shows comparisons of the VFM pressure reconstructions with transducer data at the centre point. Transducer data cannot be compared directly to

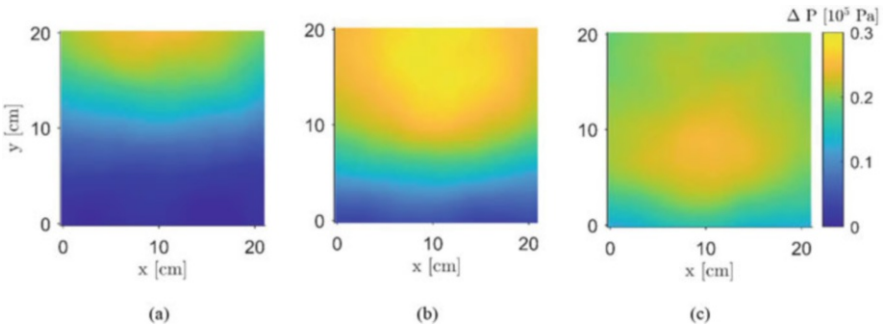

Fig. 3.4 Pressure reconstructions for half-blocked nozzle exit test case (blockage of bottom half). Reconstruction at t = 0.1 ms (**a**), t = 0.14 ms (**b**), t = 0.18 ms (**c**)

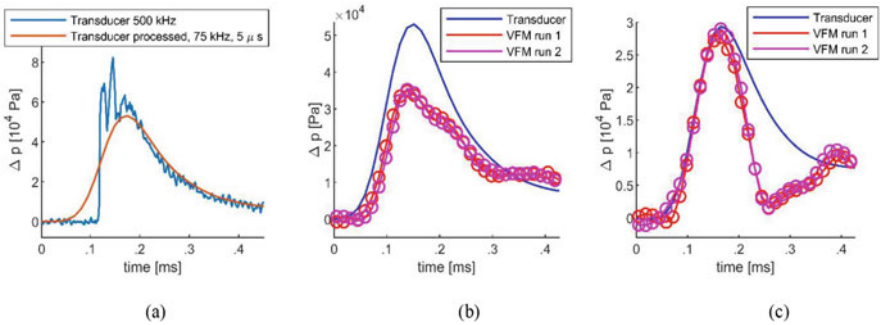

Fig. 3.5 (**a**) Original pressure transducer signal compared to processed signal to match camera frame rate of 75 kHz and shutter speed of 5 μs. Comparison between VFM and transducer data for (**a**) open and (**b**) half-blocked nozzle exit test case

optical measurement results because they record data at one point in time, while camera images are integrated over a time interval given by the shutter speed. Therefore, transducer data were recorded at 500 kHz and then averaged over intervals corresponding to the shutter speed of 5 μs. The data was then undersampled to account for the frame rate of 75 kHz. Finally, the data was filtered with a gaussian 1D filter. The latter does not fully replicate the effect of the 3D filter used on deflectometry data but should allow for a reasonable comparison. Figure 3.5a shows the original and the processed transducer signal. The originally observed, almost instantaneous rise in pressure is smoothed out, as well as some events that occur in very short time intervals.

For the open nozzle case, Fig. 3.5b shows a large discrepancy between the peak amplitudes identified with both methods. Figure 3.5c shows good agreement of peak pressures for both measurement techniques for the case of the half-blocked nozzle exit until few data point after peak pressure occurs. The amplitude reduces more quickly after the initial impact for VFM data after that point. This is likely to vibrations occurring in the setup due to the impact. The reason for the observed differences in peak amplitude for the open nozzle case is likely that the pressure transducer processing procedure makes the simplified assumption that the signal sampled at 500 kHz corresponds to a 2 μs integration time when compared to camera measurements. In practice the transducers record a single event that occurs during 2 μs almost instantaneously, thus leading to aliasing. In the half-blocked nozzle case, lower peak pressures occur such that the effect is much less noticeable. Both VFM and transducer results were found to be repeatable, such that random noise can be ruled out as reason for the discrepancy. At this point it is also important to recall that the VFM reconstruction at each point is based on a square window of 30 data points side length which are in turn being filtered with a gaussian window of 12 data points side length in both space and time. The 50 mm distance between two transducers corresponds to approximately 18 data points. The necessary space-time filtering is likely that particularly acceleration information is smeared out, and thus the governing factor for the short-time dynamics. The fact that Figs. 3.3 and 3.4 show that the pressure distributions are captured qualitatively well over several time steps for both investigated symmetries supports the argument that the deviation between transducer and VFM data is likely due to the intrinsic differences in sampling of the techniques. This issue will be investigated further in future studies.

3.6 Conclusion

This work investigates the applicability of a pressure reconstruction approach utilizing deflectometry measurements and the VFM to a shock tube environment. The shapes of the pressure fields induced by shock waves with different symmetries impacting a thin steel plate in pure bending were reconstructed. Comparisons of the amplitudes to local transducer measurements revealed significant discrepancies in peak amplitudes for some cases. This is likely because the transducer data points are recorded almost instantaneously while camera images are integrated over time intervals given by the shutter speed. Further, previous studies have found that the obtained amplitudes are very sensitive to the chosen reconstruction parameters as they influence how experimental noise and potential systematic error interfere with the signal. The 3D filter that is required to obtain sufficiently smooth acceleration maps is likely to have reduced the local acceleration amplitudes which are encoded in the short-time variations of the deflection field. This issue will be investigated further by simulating both the experiment and the measurement process. This is the only way to analyse the exact influence of filtering on the noisy acceleration and curvature maps that are used for pressure reconstruction. More transducer and deflectometry measurements will also be conducted to identify possible error sources and further explore the capabilities of the methodology presented herein.

Acknowledgements This work has been carried out with the financial support from NTNU and the Research Council of Norway (RCN) through the Centre for Advanced Structural Analysis (CASA), Centre for Research-based Innovation (RCN Project No. 237885); SINTEF Ocean and the SLADE KPN project (RCN Project No. 294748); and the Norwegian Ministry of Justice and Public Security.

References

1. Rigby, S., Tyas, A., Clarke, S.: Observations from preliminary experiments on spatial and temporal pressure measurements from near-field free air explosion. Int J Protect Struct. **6**(2), 175–190 (2015)
2. Aune, V., Valsamo, G., Casadei, F., Langseth, M., Børvik, T.: Fluid-structure interaction effects during the dynamic response of clamped thin steel plates exposed to blast loading. Int. J. Mech. Sci. **195**, 106263 (2021)
3. de Kat, R., van Oudheusden, B.: Instantaneous planar pressure determination from PIV in turbulent flow. Exp. Fluids. **52**(5), 1089–1106 (2012)
4. J. Schneiders, S. A. Caridi. F. Scarano, "Large-scale volumetric pressure from tomographic PTV with HFSB tracers," Exp Fluids 57(11): 164, 2016
5. Beverley, J., McKeon, R.: Springer Handbook of Experimental Fluid Mechanics, pp. 188–208. Springer, Berlin (2007)
6. McKeon, R.: Springer Handbook of Experimental Fluid Mechanics. Springer, Berlin, Heidelberg (2007)
7. Timoshenko, S., Woinowsky-Krieger, S.: Theory of Plates and Shells. McGraw-Hill, New York (1959)
8. Pierron, F., Gédiac, M.: The Virtual Fields Method. Extracting Constitutive Mechanical Parameters from Full-Field Deformation Measurements. Springer, New York (2012)
9. Surrel Y.: Deflectometry: a simple and efficient noninterferometric method for slope measurement (2004)
10. O'Donoughue, P., Robin, O., Berry, A.A.: Time-resolved identification of mechanical loadings on plates using the virtual fields method and deflectometry measurements. Strain. **54**, e12258 (2017)
11. Kaufmann, R., Pierron, F., Ganapathisubramani, B.: Full-field surface pressure reconstruction using the virtual fields method. Exp. Mech. **59**(8), 1203–1221 (2019)
12. Kaufmann, R., Ganapathisubramani, B., Pierron, F.: Reconstruction of surface-pressure fluctuations using deflectometry and the virtual fields method. Exp Fluids. **61**, 1–15 (2020)
13. Kaufmann, R., Ganapathisubramani, B., Pierron, F.: Surface pressure reconstruction from phase averaged deflectometry measurements using the virtual fields method. Experiment Mech. **60**, 379–392 (2019)
14. Badulescu, C., Grédiac, M., Mathias, J.D.: Investigation of the grid method for accurate in-plane strain measurement. Measurement Sci Technol. **20**, 095102 (2009)
15. Balzer, J., Werling, S.: Principles of shape from specular reflection. Measurement. **43**(10), 1305–1317 (2010)
16. Aune, V., Fagerholt, E., Langseth, M., Børvik, T.: A shock tube facility to generate blast loading on structures. Int J Protect Struct. **7**(3), 340–366 (2016)